Performance Analysis of Ternary Composites with Lignin, Eucalyptus Fiber, and Polyvinyl Chloride

Lei Wang,[a,b] Chunxia He,[a,b] Xiaolin Li,[a,b] and Xin Yang [a,b]

To investigate the feasibility of replacing eucalyptus fiber with lignin, ternary composites (Lignin/Eucalyptus fiber/Polyvinyl chloride) were prepared by extrusion molding, and the effect of the lignin content on the wood-plastic composites was studied. The microstructure, functional groups, creep behavior, and thermal behavior of the ternary composites were analyzed. The results showed that the tensile strength, flexural strength, and impact strength decreased with an increasing lignin content, whereas, the water absorption, creep resistance, hardness, and heat resistance of the ternary composites improved.

Keywords: Ternary composites; Microstructure; Functional groups

Contact information: a: College of Engineering Nanjing Agricultural University, Nanjing 210031, China;
b: Key Laboratory of Intelligence Agricultural Equipment of Jiangsu Province, Nanjing 210031, China;
** Corresponding author: chunxiahe@hotmail.com*

INTRODUCTION

Wood-plastic composites (WPCs) containing different proportions of wood fiber and plastic exhibit high strength and corrosion resistance, and excellent anti-aging, mechanical, and thermal properties. Many researchers have performed detailed studies on WPCs, which are increasingly used in various fields, such as building materials, furniture, and logistics packaging (Ayrilmis *et al.* 2012; Naseem *et al.* 2016; Nunes *et al.* 2017). Lignin is widely found in a variety of plants and is the most abundant organic substance in the world after cellulose (Pinto *et al.* 2010; Thevenot *et al.* 2010; Kijima *et al.* 2011; Yang *et al.* 2014; Zeng *et al.* 2014). Previous studies have shown that lignin not only can enhance the viscosity of composite materials, but also it can be used as a slushing agent in concrete (Barzegari *et al.* 2012; Maldhure *et al.* 2012). However, most lignin is currently discarded and not put to industrial use. Finding better uses for lignin in WPCs has thus become a research topic of interest.

Many researchers have studied the structure and characteristics of lignin. Gregorová *et al.* (2006) studied the anti-aging properties of lignin in rubber composites. Setua *et al.* (2000) produced composites by mixing modified lignin and nitrile rubber blends, and the results showed that lignin can enhance the elongation at break, hardness, and thermal stability. Abdul Khalil *et al.* (2011) improved the thermal stability and compatibility of WPCs by mixing epoxy resin and different mass ratios of oil palm shell black liquor lignin. Wood *et al.* (2011) confirmed that the impact, tensile, and flexural strengths of hemp/epoxy composites increased with the addition of lignin. Chen *et al.* (2014) analyzed Lignin/Thermoplastic composite materials by using three methods of compatibilization. Kim *et al.* (2014) described the latest research progress in the field of lignin, and proposed future research directions. Thakur *et al.* (2014) elaborated on the development status of lignin as an absorbent and membrane material. The modification of lignin has been widely investigated, but lignin has rarely been studied as a reinforcement in WPCs.

The goals of this paper were to evaluate the feasibility of replacing eucalyptus fiber with lignin in WPCs, thereby improving the recycling rate of lignin, and to analyze the effects of different proportions of lignin on the creep, mechanical, and thermal properties of the WPCs.

EXPERIMENTAL

Materials

The polyvinyl chloride (PVC) powder was purchased from Xinjiang Tianye Group Co. Ltd. (SG-5, Xinjiang, China). The lignin was purchased from Shandong Longli Biotechnology Co. Ltd. (Shandong, China) (cellulose ≤ 3%; purity ≥ 80%; and particle size = 2.9 µm to 4.3 µm) (Fig. 1). The eucalyptus fiber powder, H-108 PE wax, and non-toxic 603 Ca/Zn composite stabilizers were purchased from Shanghai Wenhua Chemical Pigment Co. Ltd. (Shanghai, China). The maleic anhydride-grafted PVC was purchased from Dongguan Lok Wah Plastic Chemical Co. Ltd. (Guangdong, China).

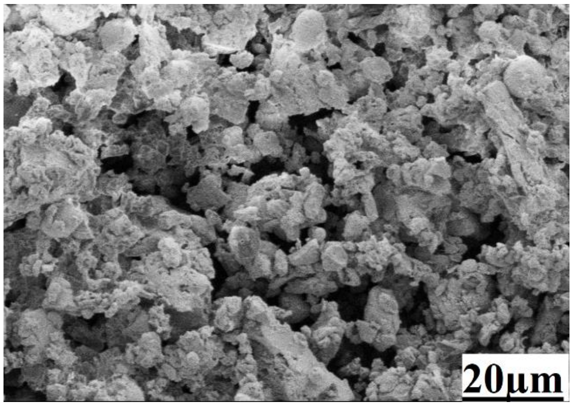

Fig. 1. Microstructure of the lignin

Sample Preparation

The eucalyptus fiber powder and waste lignin were initially crushed and subsequently ground to pass through a 100-mesh screen. They were then dried at 90 °C for 12 h in a DHG-9140A electro-thermostatic drum-wind drying oven (Nanjing Dongmai Scientific Instrument Co. Ltd., Jiangsu, China) to remove excess moisture. The lignin, eucalyptus fiber, and PVC were mixed at different ratios in an SBH-5L 3D linkage mixer (Nanjing Xinbao Mechanical and Electrical Industry Co. Ltd., Jiangsu, China). Simultaneously, 8 wt% stabilizer, 5 wt% PE wax, and 3 wt% maleic anhydride-grafted PVC (with respect to the total PVC) were added, and then placed into a RM200C conical twin-screw extruder (Harbin Hapro Electric Technology Co. Ltd., Heilongjiang, China). The temperature profiles of the four processing zones were 150 °C, 155 °C, 160 °C, and 165 °C, and the rotational speed of the screw was 20 rpm. The extruded material was cooled and the samples were cut to the dimensions 100 mm × 10 mm × 7 mm using a cutting machine (GTA600, Robert Bosch Co., Ltd, Shanghai, China).

Table 1. Formulations of the Composites

Sample ID	1	2	3	4
PVC (wt%)	50	50	50	50
Eucalyptus fiber powder (wt%)	45	40	35	0
Lignin (wt%)	5	10	15	50
Stabilizer (wt%)	8	8	8	8
PE wax (wt%)	5	5	5	5
Maleic anhydride (PVC) (wt%)	3	3	3	3

Note: 8 wt% stabilizer, 5 wt% PE wax, and 3 wt% maleic anhydride-grafted PVC were added with respect to the total PVC.

Characterization

Surface structure of the composites

Analysis of the internal structure of the composites was performed using scanning electron microcopy (SEM; S-4800, Hitachi Ltd., Tokyo, Japan). Prior to the SEM analysis, the surfaces of the PVC composites were sprayed with gold using an E-1010 ion sputter coater (S-480, Hitachi Ltd, Tokyo, Japan).

Thermal properties of the composites

The thermogravimetric (TG) analysis of the composites was performed using a STA449F3 synchronous thermal analyzer (NETZSCH Scientific Instrument Trading Co. Ltd., Bavaria, Germany). To obtain the TG curves of the composites, the pyrolysis behavior of the samples was analyzed. The measurements were performed under an argon atmosphere at a flow rate of 20 mL/min, and the samples were placed in an Al_2O_3 crucible. The temperature was increased from 30 °C to 800 °C at a heating rate of 20 °C/min, and the initial sample weight was 5 mg to 10 mg.

Functional groups of the composites

A Nicolet iS10 Fourier-transform infrared (FTIR) spectrometer (Thermo Fisher Scientific Co. Ltd., Waltham, MA, USA) was used to observe the transformation of the chemical structures in the ternary composites. The equipment was operated from 400 cm^{-1} to 4000 cm^{-1} with a resolution of 4 cm^{-1}, and each spectrum was obtained using 16 scans in the absorbance mode. There were three operational steps in the procedure. First, the equipment and FTIR software were opened and a background spectrum without a sample was obtained. Second, the samples were placed in the machine and the scans were completed. Third, the results were saved and analyzed.

Physical and mechanical properties

The hardness of the ternary composites was measured using an XHR-150 plastic Rockwell hardness tester (Shanghai Joint Seoul Test Equipment Co. Ltd., Shanghai, China) according to the Chinese standard GB/T 3398.1 (2008), and was calibrated with a ruler. The indenter diameter was 12.7 mm, the external loading was 60 kg, the load time was 5 s, and the average unloading time was 15 s. The tests were performed at room temperature.

The mechanical properties of the composites were measured using a CMT6104 electronic universal testing machine (MTS Industrial Systems Co. Ltd., Shanghai, China). The tensile, bending, and impact strengths of the ternary composites were measured according to GB/T 1040.1 (2006), GB/T 9341 (2008), and GB/T 1043.1 (2008), respectively. The test speed was 2 mm/min, and testing was performed at room temperature.

The water absorption tests were performed according to GB/T 17657 (2013). First, the samples were dried at 90 °C for 12 h to eliminate water and they were weighed with an electronic balance. Then, the samples were immersed in distilled water at 23 °C ± 1 °C for 24 h. The samples were then removed, the surfaces were wiped using blotting paper, and the samples were weighed again. The water absorption was calculated with Eq. 1,

$$c = \frac{(W_1 - W_0)}{W_0} \times 100 \tag{1}$$

where c is the water absorption (%), and W_0 and W_1 are the dry weight (g) and weight after 24 h (g), respectively.

Short-term creep tests were performed using a three-point bending test according to the Chinese standard GB/T 9341 (2008) with a UTM4104X electronic universal testing machine (Shenzhen Suns Technology Stock Co. Ltd., Shenzhen, China) at 3.11 MPa, 6.22 MPa, and 9.33 MPa. The test time was 4 h. The short-term creep tests of the four formulation samples were performed at room temperature. For accurate results, all of the samples were tested five times and the results were averaged.

RESULTS AND DISCUSSION

Physical and Mechanical Properties of the Composites

The mechanical properties of the composites are shown in Figs. 2, 3, and 4. The tensile, flexural, and impact strengths showed an obvious decrease with an increasing lignin content, and decreased by 28.2%, 21.9%, and 34%, respectively, when comparing Sample 4 with Sample 1. The fluidity of the composites was affected and the two-phase combination of eucalyptus fiber and PVC was destroyed when the eucalyptus fiber was replaced with lignin (Ago *et al.* 2012).

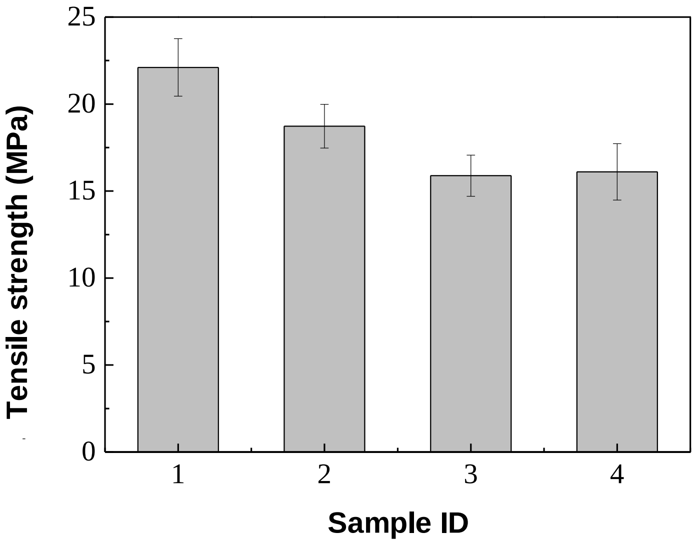

Fig. 2. Tensile strength of the composites

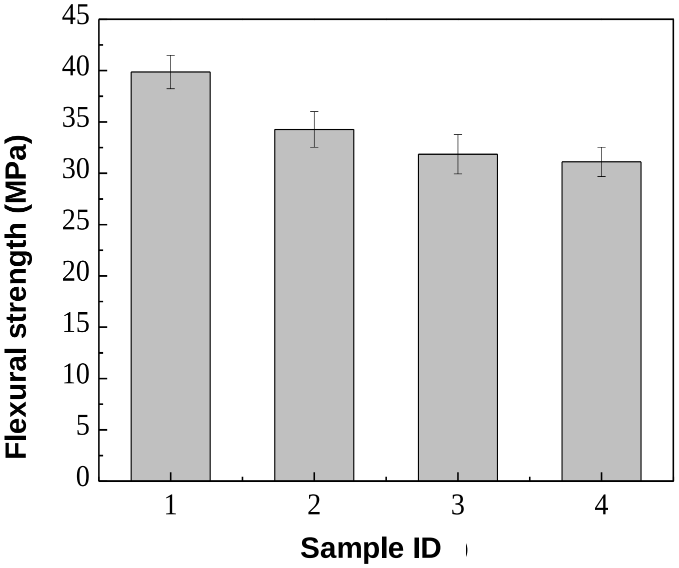

Fig. 3. Flexural strength of the composites

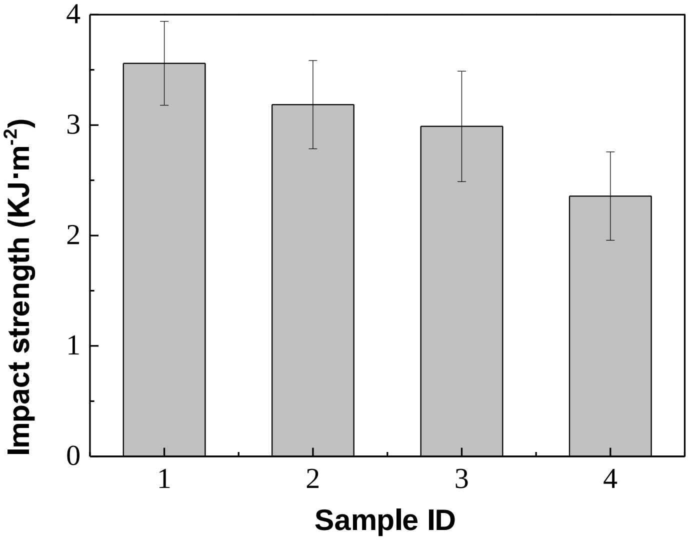

Fig. 4. Impact strength of the composites

Lignin is a rigid macromolecule and, as the proportion of eucalyptus fiber continuously decreased, it affected the integrity of the PVC matrix. Aromatic rings affect the flexibility of composites and result in non-uniform internal mixing (Liu *et al.* 2015; Lazić *et al.* 2018).

As shown in Figs. 5 and 6, the water absorption and hardness of Sample 4 increased by 80% and 41.8%, respectively, compared with Sample 1. These increases may have been a result of the large number of hydroxyl and other hydrophilic groups in the lignin. The water absorption rate of the samples increased. As the ability to assimilate water improved, it interfered with the bonding between the fiber and plastic, resulting in more micro-cracks (Korbag and Saleh 2016; Dai *et al.* 2018), and it was not easy to form tight interfacial bonding. The hardness was influenced by the rigidity of the lignin, which has a greater hardness than fiber (Jia *et al.* 2016). The addition of lignin increased the hardness of the composites. However, the addition of lignin also led to poor interfacial bonding, and micro-cracks were observable at the interface. The surface structure of composites is revealed in the SEM images (Fig. 10).

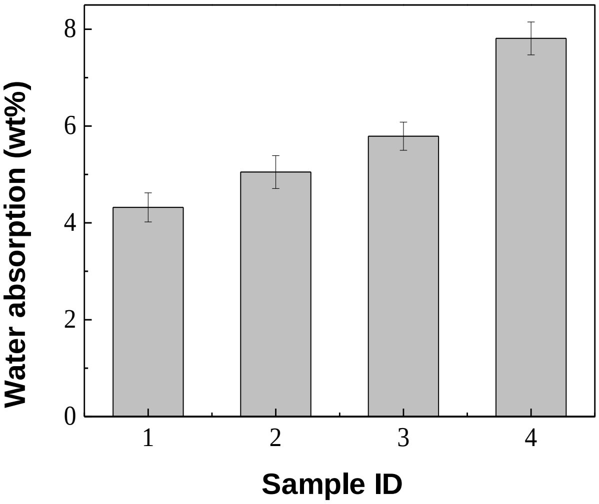

Fig. 5. Water absorption of the composites

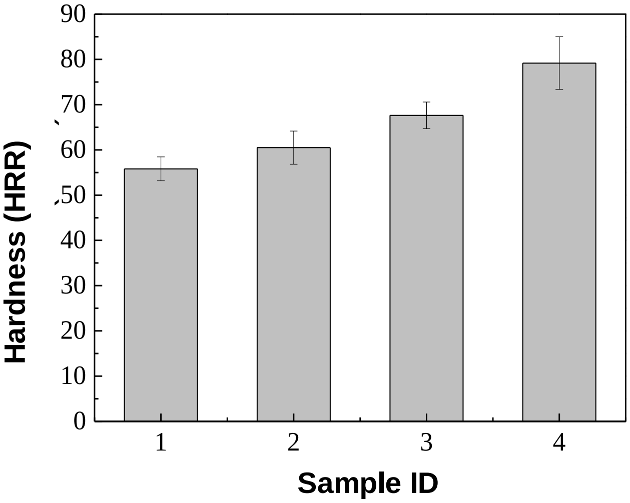

Fig. 6. Hardness of the composites

Short-term creep curves for the three different loads are shown in Figs. 7, 8, and 9. The deformation of the composites began with a sharp increase, followed by a more gradual increase. The amount of deformation correlated with the amount of external load; when the external load was larger, the deformation was larger. With a lignin content of up to 15%, the strain of the composites became less as the amount of lignin increased. The strain increased to 0.0011, 0.0017, and 0.0020 for the external loads of 3.11 MPa, 6.22 MPa, and 9.33 MPa, respectively. This may have been because of a chemical reaction between the lignin and PVC, strong two-phase bonding between the PVC and eucalyptus fiber, and improvement of the ternary composite bonding. When all of the eucalyptus fiber was replaced (Sample 4), the strain of the composite was much higher. The short-term creep performance of the ternary composites was improved with a proper amount of lignin, and then declined with excess lignin (Durán *et al.* 2016; He *et al.* 2016; Dörrstein *et al.* 2018).

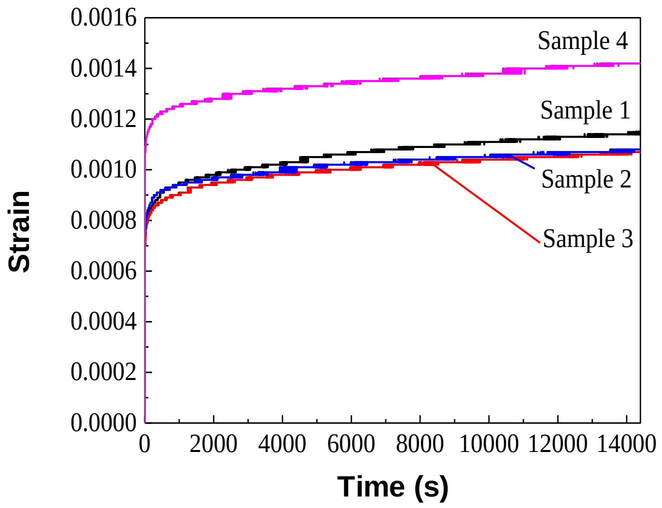

Fig. 7. Strain curves of the composites at an external load of 3.11 MPa

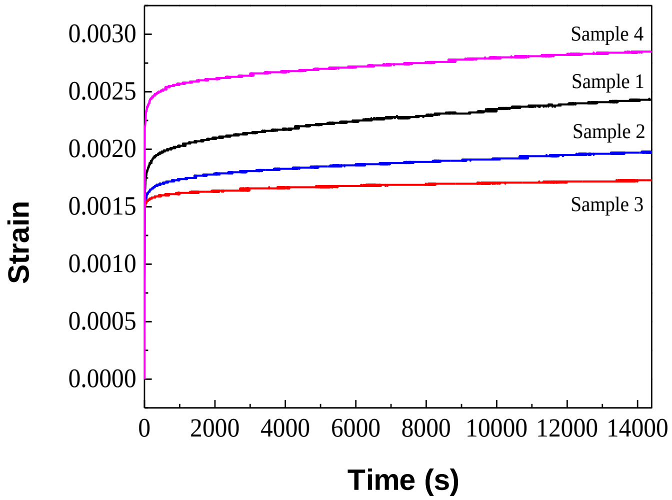

Fig. 8. Strain curves of the composites at an external load of 6.22 MPa

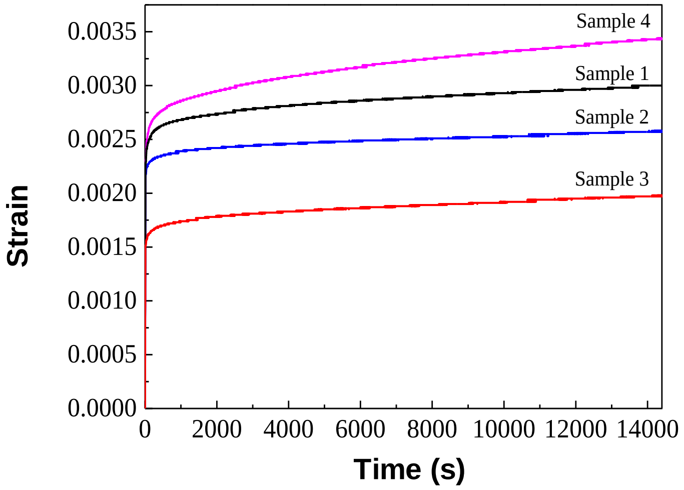

Fig. 9. Strain curves of the composites at an external load of 9.33 MPa

The microstructure of the surface under tensile fracture is shown in Fig. 10. Sample 1 appeared to have a relatively tight structure, with almost no visible holes or micro-cracks (Fig. 10a). In Sample 2, the gap between the fiber and matrix expanded, less micro-cracks occurred, and individual fibers began to separate from the matrix (Fig. 10b). In Sample 3, fibers were slowly pulled out from the matrix because of weaker intermolecular bonding, and the gaps became larger, which increased the water absorption. The structure of the ternary composite was looser, and the ability to absorb energy lessened (Fig. 10c). When the eucalyptus powder was replaced entirely with lignin in Sample 4, a two-phase structure existed and the tensile strength improved because of good dispersion. Here, the fibers completely pulled out from the matrix, which caused the appearance of a large number of holes (Fig. 10d). Because such a composite cannot absorb external energy, the mechanical properties decreased.

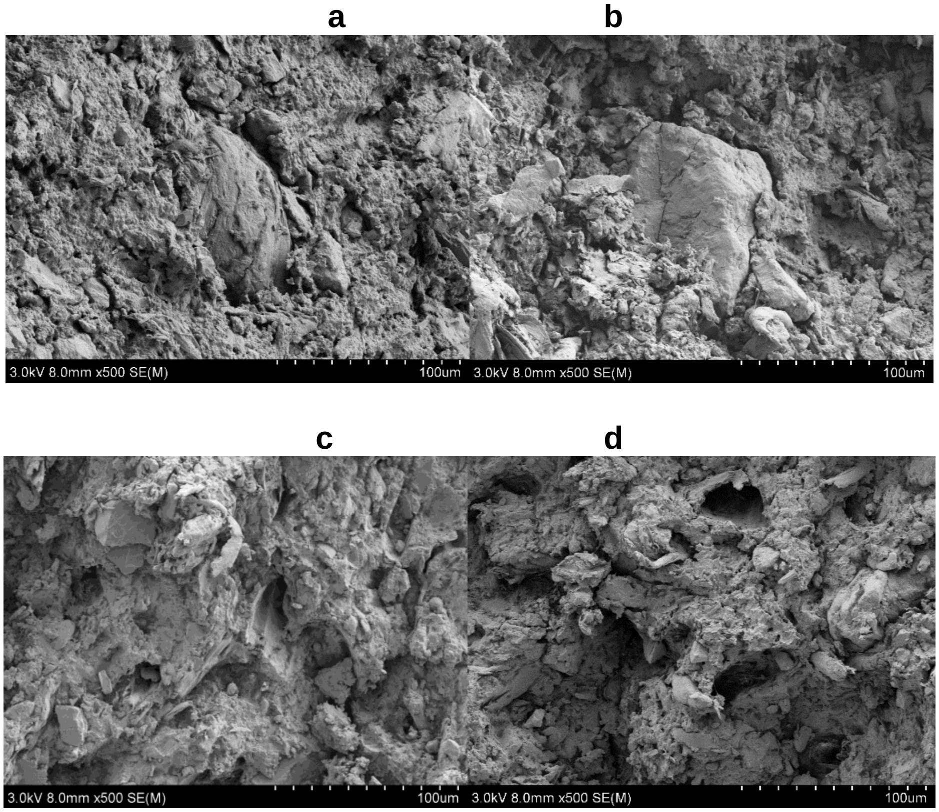

Fig. 10. Microstructure of the composites: (a) Sample 1, (b) Sample 2, (c) Sample 3, and (d) Sample 4

Infrared spectroscopy was used to analyze the ternary composites. The results are shown in Fig. 11. The main absorption peaks of the composites included 3410 cm^{-1} to 3420 cm^{-1} (stretching vibration of –OH in the hemicellulose and cellulose), 2850 cm^{-1} to 2930 cm^{-1} (asymmetric stretching vibration of C-H in the cellulose, mainly $-CH_3-$ and $–CH_2-$), 1710 cm^{-1} to 1745 cm^{-1} (C-O stretching vibration of carbonyl groups and non-conjugated carbonyl groups in the lignin and hemicellulose), and 1737 cm^{-1} (C-O stretching vibration of maleic anhydride). It has been reported that maleic anhydride can effectively graft with the PVC, such that PVC-g-MAH and eucalyptus powder can be better combined, resulting in better interfacial compatibility (Zhang *et al*. 2016). Other absorbances were 1230 cm^{-1}

to 1250 cm^{-1} (C-O stretching vibration in the lignin), 990 cm^{-1} to 1100 cm^{-1} (C-O stretching vibration in the cellulose), and 600 cm^{-1} to 700 cm^{-1} (C-Cl stretching vibration in the PVC). The -OH content gradually increased as well, which resulted in a higher polarity of the intermolecular bonding. Bonding between the fiber and plastic was difficult, and therefore the mechanical properties declined and water absorption increased. The overall results made it clear that the ternary composites with different chemical components had similar chemical functional groups, which indicated that new groups were not generated. Other researchers drew similar conclusions about the infrared absorption characteristics of composites with lignin (Yuan *et al.* 2011; Sun *et al.* 2017).

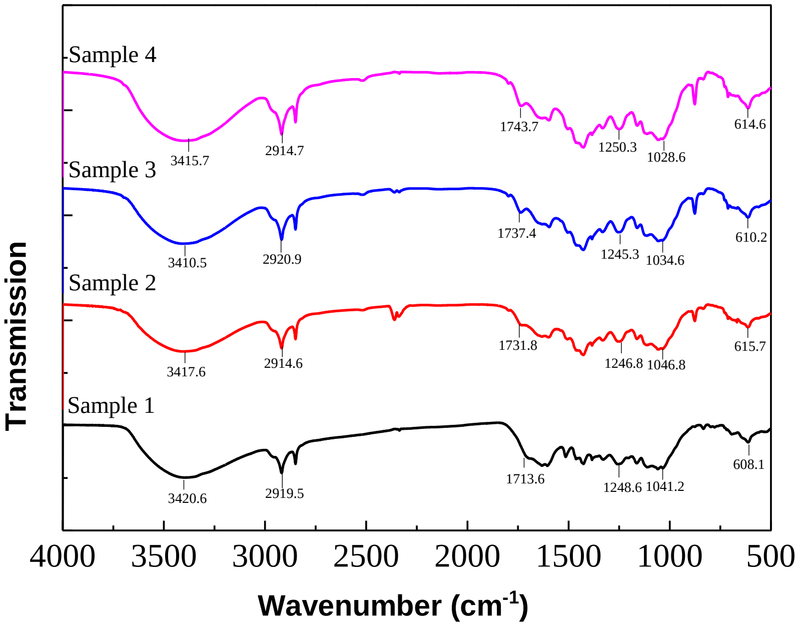

Fig. 11. FTIR spectra of the composites

The thermal properties of composites are important for real-life applications. The TG curves of the composites containing different lignin contents were obtained and are shown in Fig. 12. The curves were analyzed and the TG parameters were obtained for each of the four samples. Sample 4 had the highest temperatures for each of the decomposition phases (Table 2). The thermal stability of the composites improved with an increase in the lignin content, which was attributed to the lignin structure. As a three-dimensional polymer, lignin has a relatively high molecular weight, which makes its thermal properties more stable than those of other materials.

Table 2. Pyrolysis Temperature of the Composites

Sample ID	Pyrolysis Temperature (°C)			
	First Stage		Second Stage	
	Onset	Termination	Onset	Termination
1	260.5	324.1	446	475.6
2	261.2	325.6	447.4	477.8
3	262.5	326.6	448.3	477.9
4	271.6	327	450.9	480

The weight loss of the composites was mainly divided into three stages. The first stage occurred below 100 °C, which included the evaporation of free water molecules and relatively low-mass molecules. The most important stage during the TG process was the second stage, which occurred between 260 °C and 330 °C, in which the α-aryl and β-aryl ether bonds were broken in the lignin. Dehydration and decarboxylation reactions also occurred during this stage. A third stage occurred between 445 °C and 480 °C, in which Cl was removed from the PVC matrix by breaking the C-Cl bonds to form HCl. When the temperature reached 500 °C, the residual materials began to pyrolyze and volatilize (Ramiah 1970; Xiao *et al.* 2001; Sen *et al.* 2015). The thermal properties of the ternary composites were improved by adding lignin, which establishes a foundation for deeper analysis and application of these composites.

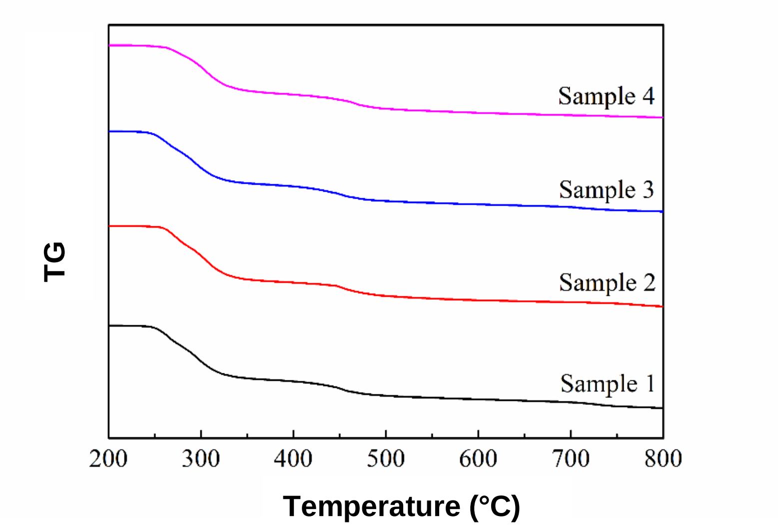

Fig. 12. TG curves of the composites

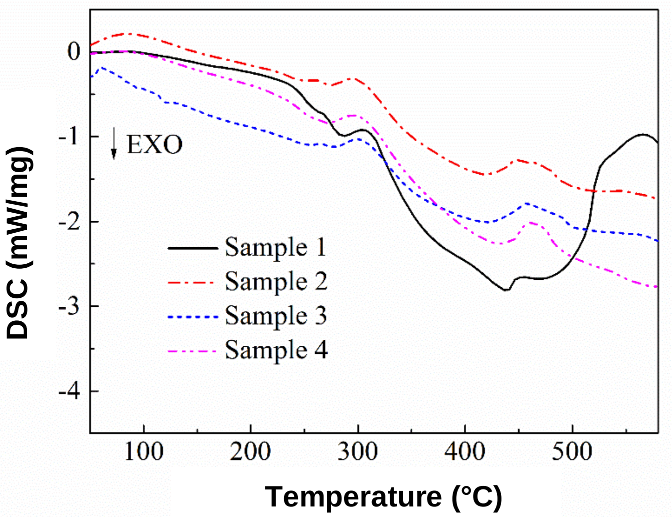

Fig. 13. Differential scanning calorimetry (DSC) curves of the composites

The effects of differential scanning calorimetry curves of the composites are shown in Fig. 13. Between 50 °C and 100 °C, an endothermic peak occurred in the four composites, mainly because of moisture or small molecular species that escaped from the fiber and matrix. An endothermic peak appeared between 200 °C and 250 °C, in which heat was absorbed during the dehydration reaction. Two exothermic peaks occurred between 250 °C and 480 °C; Cl was removed from the PVC in this temperature range. Above 500 °C, an endothermic peak occurred, in which the carbon residue aggregated because of heat absorption by the remaining substances.

CONCLUSIONS

1. This study investigated ternary composites prepared by extrusion molding. Their creep and thermal behavior at different lignin contents, as well as their mechanical and thermal properties, were analyzed. Their mechanical properties became less favorable with the addition of lignin, except for the creep resistance and hardness.
2. Thermal behavior improved with the addition of lignin. No new groups were generated when the formulation was changed. The thermal decomposition trends for the ternary composites were similar. The heat resistance of the ternary composites gradually increased with the lignin content. The use of lignin in composites helps to recycle resources. Most importantly, lignin can be utilized instead of becoming a waste product.
3. The addition of lignin led to a deterioration of interfacial bonding.

ACKNOWLEDGEMENTS

This work was supported by the National Key Technology Support Program (2011BAD20B202-2, Nanjing, China).

REFERENCES CITED

Abdul Khalil, H. P. S., Marliana, M. M., Issam, A. M., and Bakare, I. O. (2011). "Exploring isolated lignin material from oil palm biomass waste in green composites," *Mater. Design* 32(5), 2604-2610. DOI: 10.1016/jmatdes.2011.01.035

Ago, M., Okajima, K., Jakes, J. E., Park, S., and Rojas, O. J. (2012). "Lignin-based electrospun nanofibers reinforced with cellulose nanocrystals," *Biomacromolecules* 13(3), 918-926. DOI: 10.1021/bm201828g

Ayrilmis, N., Benthien, J. T., and Thoemen, H. (2012). "Effects of formulation variables on surface properties of wood plastic composites," *Compos. Part B-Eng.* 43(2), 325-331. DOI: 10.1016/j.compositesb.2011.07.011

Barzegari, M. R., Alemdar, A., Zhang, Y. L., and Rodrigue, D. (2012). "Mechanical and rheological behavior of highly filled polystyrene with lignin," *Polym. Composite.* 33(3), 353-361. DOI: 10.1002/pc.22154

Chen, F., Zhao, Y., Feng, Y., and Qu, J. (2014). "Progress of interfacial compatibilization methods of lignin/thermoplastic composites," *CIESC J.* 65(3), 777-784. DOI: 10.3969/j.issn.0438-1157.2014.03.002

Dai, Z., Shi, X., Liu, H., Li, H., Han, Y., and Zhou, J. (2018). "High-strength lignin-based carbon fibers *via* a low-energy method," *RSC Adv.* 8(3), 1218-1224.

DOI: 10.1039/C7RA10821D

Dörrstein, J., Scholz, R., Schwarz, D., Schieder, D., Sieber, V., Walther, F., and Zollfrank, C. (2018). "Effects of high-lignin-loading on thermal, mechanical, and morphological properties of bioplastic composites," *Compos. Struct.* 189, 349-356. DOI: 10.1016/j.compstruct. 2017.12.003

Durán, V. L., Larsson, P. A., and Wågberg, L. (2016). "On the relationship between fibre composition and material properties following periodate oxidation and borohydride reduction of lignocellulosic fibres," *Cellulose* 23(6), 3495-3510. DOI: 10.1007/s10570-016-1061-4

GB/T 1040.1 (2006). "Plastics - Determination of tensile properties – Part 1: General principles," Standardization Administration of China, Beijing, China.

GB/T 1043.1 (2008). "Plastics - Determination of impact properties – Part 1: Non-instrumented impact test," Standardization Administration of China, Beijing, China.

GB/T 17657 (2013). "Test methods of evaluating the properties of wood-based panels and surface decorated wood-based panels," Standardization Administration of China, Beijing, China.

GB/T 3398.1 (2008). "Plastics - Determination of hardness – Part 1: Ball indentation method," Standardization Administration of China, Beijing, China.

GB/T 9341 (2008). "Plastics - Determination of flexural properties," Standardization Administration of China, Beijing, China.

Gregorová, A., Košiková, B., and Moravčik, R. (2006). "Stabilization effect of lignin in natural rubber," *Polym. Degrad. Stabil.* 91(2), 229-233. DOI: 10.1016/j.polymdegradstab.2005.05.009

He, S., Liu, T., and Di, M. (2016). "Preparation and properties of wood flour reinforced lignin-epoxy resin composite," *BioResources* 11(1), 2319-2333. DOI: 10.15376/biores.11.1.2319-2333

Jia, Z., Lu, C., Liu, Y., Zhou, P., and Wang, L. (2016). "Lignin/polyacrylonitrile composite hollow fibers prepared by wet-spinning method," *ACS Sustain. Chem. Eng.* 4(5), 2838-2842. DOI: 10.1021/acssuschemeng.6b00351

Kijima, M., Hirukawa, T., Hanawa, F., and Hata, T. (2011). "Thermal conversion of alkaline lignin and its structured derivatives to porous carbonized materials," *Bioresour. Technol.* 102(10), 6279-6285. DOI: 10.1016/j.biortech.2011.03.023

Kim, J.-Y., Hwang, H., Oh, S., Kim, Y.-S., Kim, U.-J., and Choi, J. W. (2014). "Investigation of structural modification and thermal characteristics of lignin after heat treatment," *Int. J. Biol. Macromol.* 66, 57-65. DOI: 10.1016/j.ijbiomac.2014.02.013

Korbag, I., and Saleh, S. M. (2016). "Studies on the formation of intermolecular interactions and structural characterization of polyvinyl alcohol/lignin film," *Int. J. Environ. Stud.* 73(2), 226-235. DOI: 10.1080/00207233.2016.1143700

Lazić, B. D., Pejić, B. M., Kramar, A. D., Vukčević, M. M., Mihajlovski, K. R., Rusmirović, J. D., and Kostić, M. M. (2018). "Influence of hemicelluloses and lignin content on structure and sorption properties of flax fibers (*Linum usitatissimum* L.)," *Cellulose* 25(1), 687-709. DOI: 10.1007/s10570-017-1575-4

Liu, H. C., Chien, A.-T., Newcomb, B. A., Liu, Y., and Kumar, S. (2015). "Processing, structure, and properties of lignin- and CNT-incorporated polyacrylonitrile-based carbon fibers," *ACS Sustain. Chem. Eng.* 3(9), 1943-1954. DOI: 10.1021/acssuschemeng.5b00562

Maldhure, A. V., Ekhe, J. D., and Deenadayalan, E. (2012). "Mechanical properties of polypropylene blended with esterified and alkylated lignin," *J. Appl. Polym. Sci.* 125(3), 1701-1712. DOI: 10.1002/app.35633

Naseem, A., Tabasum, S., Zia, K. M., Zuber, M., Ali, M., and Noreen, A. (2016). "Lignin-derivatives based polymers, blends and composites: A review," *Int. J. Biol. Macromol.* 93(Part A), 296-313. DOI: 10.1016/j.ijbiomac.2016.08.030

Nunes, S. G., da Silva, L. V., Amico, S. C., Viana, J. D., and Amado, F. D. R. (2017). "Study of composites produced with recovered polypropylene and piassava fiber," *Materials Research* 20(1), 144-150. DOI: 10.1590/1980-5373-mr-2016-0659

Pinto, P. C. R., da Silva, E. A. B., and Rodrigues, A. E. (2010). "Comparative study of solid-phase extraction and liquid-liquid extraction for the reliable quantification of high value added compounds from oxidation processes of wood-derived lignin," *Ind. Eng. Chem. Res.* 49(23), 12311-12318. DOI: 10.1021/ie101680s

Ramiah, M. V. (1970). "Thermogravimetric and differential thermal analysis of cellulose, hemicellulose, and lignin," *J. Appl. Polym. Sci.* 14(5), 1323-1337. DOI: 10.1002/app.1970.070140518

Sen, S., Patil, S., and Argyropoulos, D. S. (2015). "Thermal properties of lignin in copolymers, blends, and composites: A review," *Green Chem.* 17(11), 4862-4887. DOI: 10.1039/C5GC01066G

Setua, D. K., Shukla, M. K., Nigam, V., Sing, H., and Mathur, G. N. (2000). "Lignin reinforced rubber composites," *Polym. Composite.* 21(6), 988-995. DOI: 10.1002/pc.10252

Sun, J., Wang, C., Stubbs, L. P., and He, C. (2017). "Carboxylated lignin as an effective cohardener for enhancing strength and toughness of epoxy," *Macromol. Mater. Eng.* 302(12), 1700341. DOI: 10.1002/mame.201700341

Thakur, V. K., Thakur, M. K., Raghavan, P., and Kessler, M. R. (2014). "Progress in green polymer composites from lignin for multifunctional applications: A review," *ACS Sustain. Chem. Eng.* 2(5), 1072-1092. DOI: 10.1021/sc500087z

Thevenot, M., Dignac, M.-F., and Rumpel, C. (2010). "Fate of lignins in soils: A review," *Soil Biol. Biochem.* 42(8), 1200-1211. DOI: 10.1016/j.soilbio.2010.03.017

Wood, B. M., Coles, S. R., Maggs, S., Meredith, J., and Kirwan, K. (2011). "Use of lignin as a compatibiliser in hemp/epoxy composites," *Compos. Sci. Technol.* 71(16), 1804-1810. DOI: 10.1016/j.compscitech.2011.06.005

Xiao, B., Sun, X. F., and Sun, R.-C. (2001). "Chemical, structural, and thermal characterizations of alkali-soluble lignins and hemicelluloses, and cellulose from maize stems, rye straw, and rice straw," *Polym. Degrad. Stabil.* 74(2), 307-319. DOI: 10.1016/S0141-3910(01)00163-X

Yang, Y., Deng, Y., Tong, Z., and Wang, C. (2014). "Renewable lignin-based xerogels with self-cleaning properties and superhydrophobicity," *ACS Sustain. Chem. Eng.* 2(7), 1729-1733. DOI: 10.1021/sc500250b

Yuan, T.-Q., Sun, S.-N., Xu, F., and Sun, R.-C. (2011). "Structural characterization of lignin from triploid of *Populus tomentosa* Carr.," *J. Agr. Food Chem.* 59(12), 6605-6615. DOI: 10.1021/jf2003865

Zeng, Y., Zhao, S., Yang, S., and Ding, S.-Y. (2014). "Lignin plays a negative role in the biochemical process for producing lignocellulosic biofuels," *Curr. Opin. Biotech.* 27, 38-45. DOI: 10.1016/j.copbio.2013.09.008

Zhang, W. -L., Zhao Y. -N., Han K. -W., and Dai Y. -J. (2016). "Preparation of chlorinated poly (vinyl chloride) grafted with maleic anhydride and its application in poly (vinyl chloride)," *China Plastics* 30(2), 49-53.

Article submitted: May 8, 2018; Peer review completed: June 28, 2018; Revised version received and accepted: July 5, 2018; Published: July 11, 2018.
DOI: 10.15376/biores.13.3.6510-6523

Erratum: March 23, 2020: Figure 12 has been updated with revised curves; page 6515, creep deformation was changed to 0.0017 from 0.0016. Revisions do not change the conclusions of this paper.